Journal of Computers Vol. 30 No. 3, 2019, pp. 1-13
doi:10.3966/199115992019063003001

Automatic Extraction of Fuzzy and Touching Leukocyte Using Improved FWSA K-means in Peripheral Blood and Bone Marrow Cell Images

Li-Qun Lin[1], Wei-Xing Wang[1,2*]

[1] College of Physics and Information Engineering, Fuzhou University, Fuzhou 350108, Fujian, China
t07063@fzu.edu.cn, wxwang@chd.edu.cn

[2] Royal Institute of Technology, Stockholm, Sweden

Received 7 August 2017; Revised 19 December 2017; Accepted 1 February 2018

Abstract. Due to the complexity of cell structure and the overlap of cells, accurate segmentation of cytoplasm and nucleus remains a challenging problem. Here an algorithm based on feature weight adaptive K-means clustering to extract complex leukocytes is proposed. In traditional K-means clustering algorithm, the initial clustering center is randomly assigned, which affects the clustering effect. In this paper, the initial clustering center is selected according to the histogram distribution of cell image, which not only improves the clustering effect, but also reduces the time complexity of the algorithm from O (n) to O (1). Then, the improved K-means algorithm can have some anti-noise performance by using a non-Euclidean distance · Before leukocytes are extracted, the color space is decomposed, and the cell nucleus and cytoplasm are extracted according to the color component and the improved K-means clustering algorithm. Color space decomposition and K-means clustering are combined for segmentation. Finally, Adherent leukocytes are separated based on watershed algorithm. The proposed segmentation method achieves 95.81% and 91.28% overall accuracy for nucleus and cytoplasm segmentation, respectively. Experimental results show that the new method can effectively segment complex leukocytes and have high accuracy.

Keywords: bone marrow cell images, improved FWSA-KM algorithm, K-means clustering, leukocyte extraction,

1 Introduction

White blood cells (WBCs), also called leukocytes, play an important role in the auxiliary diagnosis of various diseases, such as AIDS, leukemia, and other blood-related diseases. In the human body, the number of WBCs is usually maintained within a certain range. If the number of WBCs exceeds the normal range, then health problems may occur. In routine blood tests, the traditional counting and morphological analysis of WBCs relies on manual counting and expert analysis, with low efficiency and strong subjectivity. Therefore, the blood cell automatic analyzer, used for automatic classification count and morphological analysis of WBCs, is needed to be developed. Among them, the flow cytometry is current commonly used. However, the costly flow cytometry cannot achieve automatic classification of WBCs, which leads to its limitations in clinical applications. In recent years, the technology based on image processing and pattern recognition, with the advantage of low cost, has been gradually improved for morphology analysis and classification recognition of WBCs, and has a wide range of applications.

For the automatic classification and recognition system of WBCs, leukocyte segmentation is an important part of leukocyte classification system because the segmentation results directly affect the accuracy of cell recognition. Some effective algorithms to achieve accurate segmentation of WBC have been put forward. Zheng et al. [1] combined the expectation maximization clustering and SVM for

* Corresponding Author

WBCs segmentation. The performance of the learning-based method depends mainly on the selected color feature vector. Active contour-based methods include level set and Snake algorithm. For example, Wang et al. [2] proposed to segment the nucleus region first, and then segment the cytoplasm by gradient vector flow (GVF) Snake. The boundary of the nucleus was taken as the initial contour of the Snake algorithm. Ko et al. [3] proposed a stepwise merging method based on mean clustering and GVF Snake algorithm for WBCs segmentation. In the WBCs segmentation application, the visual significance method has a good segmentation effect. Zheng et al. [4] used a visual saliency algorithm to achieve localization and segmentation of WBCs. Pan et al. [5-6] adopted visual significance algorithm to achieve WBCs segmentation, and achieved good results. Several researchers have studied the cell segmentation with K-means shift clustering algorithm [7, 9-11], color space [8, 17-19], morphological methods [8, 12-14], watershed technique [15], and fuzzy C means cluster [16] to obtain the contours of WBCs in peripheral blood and bone marrow cell images. The algorithm relies too much on initializing data and other parameters. The clustering results are closely related to the data number and shape of the target. When the color of the cytoplasm is significantly different from the nucleus, this algorithm can not accurately obtain all WBCs in some special images.

In summary, although many methods have been proposed, majority of these methods have some defects to different extent, such as different color brightness of the image, the presence of impurities, a variety of white blood cell shape, and the similar color for stained cytoplasm and red blood cells. And so far, the segmentation accuracy of existing methods can not meet the actual clinical needs. Thus, in this paper, we present a general method for WBC segmentation based on improved K-means clustering algorithm. It can be adapted to detect WBCs in a microscopic image and segment their components, nucleus, and cytoplasm. The proposed method provided automated segmentation for WBCs with less computation time and error rate.

2 Precise Extraction of Leukocytes

2.1 Different Color Spaces

The original blood smear image is represented by the RGB color space in the RGB model. Each pixel consists of red (R), green (G) and blue (B) three color components. The three color components superimposed on different color levels, producing different colors. Therefore, at present, RGB color space is the most widely used color system. The HSI color model consists of three parts, Hue (H), Saturation (S) and Brightness (I), which are the same as the way people perceive color. Because of its low correlation with image processing, HSI space is more suitable for WBCs segmentation than RGB space. Assuming that the RGB values are normalized to the [0, 1] range, the HSI color space may be derived from RGB space conversion.

Each color space has its own characteristics, which can be used separately for color decomposition and analysis. For example, when the original blood cell image of the RGB color space is converted to the HSI color spaces, features are conducive to white blood cell division occur.

2.2 Improved FWSA K-means Clustering Algorithm

K-means clustering is one of the most classical segmentation algorithms in clustering algorithm. The algorithm is simple and fast, which makes the algorithm widely used. However, the algorithm is sensitive to the initial selection of the center point and the impact of noise, and it can not automatically select features.

Improvement of initial clustering center selection. In the K-means algorithm: for gray-scale images, the classification number is m, the selected gray value (normalized) is generally $1/m, 2/m, \cdots, 1$. According to this selection of clustering center, the time complexity of the algorithm is high. However, as shown in Fig. 2, the background gray value of the cell image is usually 0, while that of the red blood cell and the white cell cytoplasm is larger, approximately between 0.2-0.3 and 0.3-0.5, and the gray value of nucleus is greater than 0.8. If the traditional K-means algorithm is used, the algorithm needs several iterations to find the convergent center point. The time complexity of it is O (n).

In traditional K-means clustering algorithm, the initial clustering center is randomly assigned to affect the clustering effect. In this paper, the initial clustering center is selected according to the gray histogram

distribution of the cell image, and the initial clustering of all pixels in the image is carried out according to the nearest neighbor principle. Before the iteration, we only need to make the the histogram statistic of the cell image, and then use the information provided by the histogram to convert the processing of each point to the processing of each gray value, which greatly reduces the complexity of the algorithm. The time complexity is O (1).

In Fig. 1(a), for m = 3, the initialization points are 0.33, 0.66 and 1, respectively. The initial clustering center points are selected according to the gray-level histogram: 0.25, 0.5 and 0.75. It can be seen from Fig. 1(b) that the initial clustering center of the improved algorithm is closer to the gray distribution in the cell image. The gray value of each class pixels is taken as the cluster center value of the class point, and the image segmentation result is shown in Fig. 1(c).

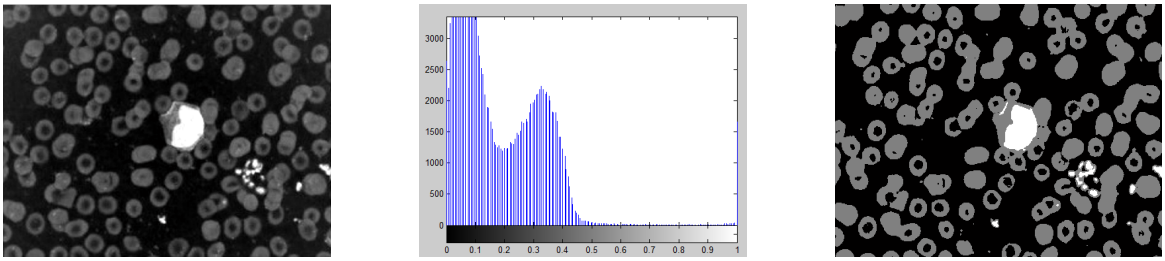

(a) Grayscale image (b) Gray histogram (c) Clustering result

Fig. 1. Improved FWSA K-means algorithm

Distance improvement. In order to achieve low anti-noise performance of clustering algorithm, Ref. [20] have proposed the feature weight adaptive computing (referred to as FWSA-KM algorithm) to improve the K-means clustering algorithm. The algorithm requires less parameter without reducing the efficiency of the algorithm, and however uses the Euclidean distance. For the noisy or complex data structure, the FWSA-KM algorithm has less clustering effect. In order to improve the robustness of the algorithm, we can improve the K-means clustering algorithm based on non-Euclidean distance, and improve the Euclidean distance $\left|\chi_{ik}-v_{jk}\right|$ of χ_{ik} and v_{jk} in the objective function of FWSA-KM algorithm to non-Euclidean distance $\sqrt{1-\exp\left\{-\gamma_k(\chi_{ik}-v_{jk})^2\right\}}$, and the objective function of the improved FWSA-KM clustering algorithm is:

$$J_{IFWSA-KM}=(U,V,W)=\sum_{i=1}^{n}\sum_{j=1}^{c}\sum_{k=1}^{m}u_{ij}w_k\left\{1-\exp[-\gamma_k(\chi_{ik}-v_{jk})^2]\right\}. \tag{1}$$

where $U=(u_{ij})_{n\times c}$ is the membership matrix. If the i-th data point x_i belongs to the j-th class, then $u_{ij}=1$, otherwise $u_{ij}=0$, and $\sum_{j=1}^{c}u_{ij}=1(i=1,2,\cdots,n)\circ$ $V=\left[v_1,v_2,\cdots,v_c\right]$ is a matrix of c clustering centers.

While the formulas are given as follows:

$$\begin{cases}\sum_{j=1}^{c}u_{ij}=1(1\le i\le n),\\ u_{ij}\in\{0,1\}(1\le j\le c,1\le i\le n),\\ \sum_{k=1}^{m}w_k=1,\\ w_k\ge 0(1\le k\le m).\end{cases} \tag{2}$$

The elements of the optimal membership matrix $\hat{U}$ and the cluster center matrix $\hat{V}$ are:

$$\hat{u}_{ij} = \begin{cases} 1, if \sum_{k=1}^{m} w_k (x_{ik} - v_{jk})^2 \leq \\ \sum_{k=1}^{m} w_k (x_{ik} - v_{jk})^2 \\ (l = 1, 2, \cdots, c); \\ 0, else. \end{cases} \tag{3}$$

$$\hat{v}_{jk} = \sum_{i=1}^{n} (u_{ij} \bullet x_{ik}) / \sum_{i=1}^{n} u_{ij} \quad . \tag{4}$$

By solving the three minimization problems iteratively, the formula (1) can be minimized.
Make,

$$a_k = \sum_{i=1}^{n} \sum_{j=1}^{c} u_{ij} \left[1 - e^{-\gamma_k (\chi_{ik} - v_{jk})^2} \right], \tag{5}$$

$$b_k = \sum_{i=1}^{n} \sum_{j=1}^{c} u_{ij} \left[1 - e^{-\gamma_k (v_{jk} - \overline{\chi_k})^2} \right]. \tag{6}$$

Among them,

$$\overline{\chi_k} = \sum_{i=1}^{n} \frac{\chi_{ik}}{n} (k = 1, 2, \ldots, m) \quad . \tag{7}$$

Then a_k measures the total intraclass compactness of the cluster on the k-dimensional feature, and b_k measures the total interclass separability measure of the cluster on the k-th dimension feature.

Here, we define a new objective function to solve the feature weight matrix.

$$\begin{aligned} &\max J_{IFWSA-KM}(\hat{U}, \hat{V}, W) = \\ &\frac{\sum_{i=1}^{n} \sum_{j=1}^{c} \sum_{k=1}^{m} u_{ij} w_k \left[1 - e^{-\gamma_k (v_{jk} - \bar{x}_k)^2} \right]}{\sum_{i=1}^{n} \sum_{j=1}^{c} \sum_{k=1}^{m} u_{ij} w_k \left[1 - e^{-\gamma_k (x_{ik} - v_{jk})^2} \right]} = \\ &\frac{\sum_{k=1}^{m} w_k \left\{ \sum_{i=1}^{n} \sum_{j=1}^{c} u_{ij} \left[1 - e^{-\gamma_k (v_{jk} - \bar{x}_k)^2} \right] \right\}}{\sum_{k=1}^{m} w_k \left\{ \sum_{i=1}^{n} \sum_{j=1}^{c} u_{ij} \left[1 - e^{-\gamma_k (x_{ik} - v_{jk})^2} \right] \right\}} = \\ &\frac{\sum_{k=1}^{m} w_k b_k}{\sum_{k=1}^{m} w_k a_k}, \end{aligned} \tag{8}$$

Satisfy,

$$\begin{cases} \sum_{k=1}^{m} w_k = 1, \\ w_k \geq 0 (k = 1, 2. \cdots, m). \end{cases} \tag{9}$$

In the FWSA-KM clustering algorithm, let $\left\{w_1^{(t)}, w_2^{(t)}, \cdots, w_m^{(t)}\right\}$ be the feature weight of the iteration in step t, then the following formula can be expressed as the feature weight of step t + 1:

$$w_k^{(t+1)} = w_k^{(t)} + \Delta w_k^{(t)} (k = 1, 2, \cdots, m), \tag{10}$$

The feature weight increment is given by

$$\Delta w_k^{(t)} = \frac{b_k^{(t)} / a_k^{(t)}}{\sum_{k=1}^{m} (b_k^{(t)} / a_k^{(t)})} (k = 1, 2, \cdots, m). \tag{11}$$

In order to make $w_k^{(t+1)}$ satisfying the constraint condition:

$$\sum_{k=1}^{m} w_k^{(t+1)} = 1. \tag{12}$$

The normalization of the formula (10) gives the weight of the feature as follows:

$$w_k^{(t+1)} = \frac{1}{2}\left[w_k^{(t)} + \Delta w_k^{(t)} \right] \quad (k = 1, 2, \cdots, m). \tag{13}$$

In summary, the algorithm consists of the following 5 steps:
Initialize the cluster center matrix

$$V^{(0)} = \{V_1, V_2, \cdots, V_C\}. \tag{14}$$

The initial feature weight matrix W satisfies:

$$W_K^{(0)} = 1/m (k = 1, 2, \cdots, m). \tag{15}$$

Calculate the membership matrix U.
The new clustering center matrix V is calculated.
The characteristic weight matrix W is calculated by the equation (13).
If

$$\max_{i,j} \left| u_{ij} - u_{ij}' \right| < \varepsilon. \tag{16}$$

The algorithm stops, otherwise go to step 2.

2.3 Extraction of Nuclei

Selection of color model. Fig. 2 is the color cell images of peripheral blood cells and bone marrow. It can be seen from the figure, the nucleus of WBCs are in purple or dark blue, with the color being darker compared with the surrounding blood cells and cytoplasm that are in red.

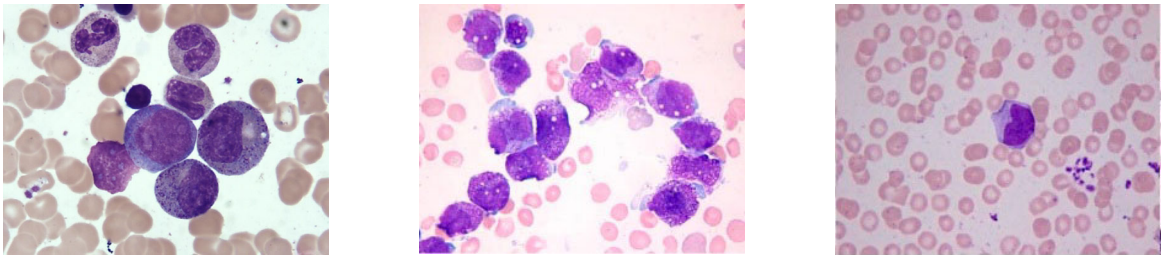

Fig. 2. Color peripheral blood cells and bone marrow cell images

It can be seen from Fig. 3 that the cytoplasmic region and the WBCs region of the hue component (H) and saturated component (S) of the treated WBCs have a strong contrast with the background image.

According to the above characteristics, in the subsequent segmentation, a suitable threshold value can be set in S component and H component to roughly extract the nucleus region and the leukocyte region from the peripheral blood cell image.

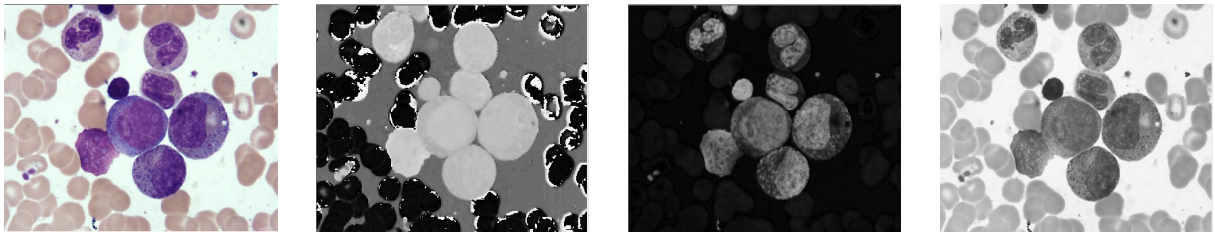

(a) Original image (b) H component (c) S component (d) V component

Fig. 3. Color spatial component

Nuclear extraction. The clustered binary image contains a large amount of noise, as shown in Fig. 4(a). Because the area of noise is small, the area of each connected area is calculated by using this feature. After the area of the connected area is less than the threshold, the denoised image is obtained, as shown in Fig. 4(b). After denoising, some small holes still occurred in the white cell nucleus area. Next, the holes were filled and the original nuclei morphology of the WBCs was restored, as shown in Fig. 4(c).

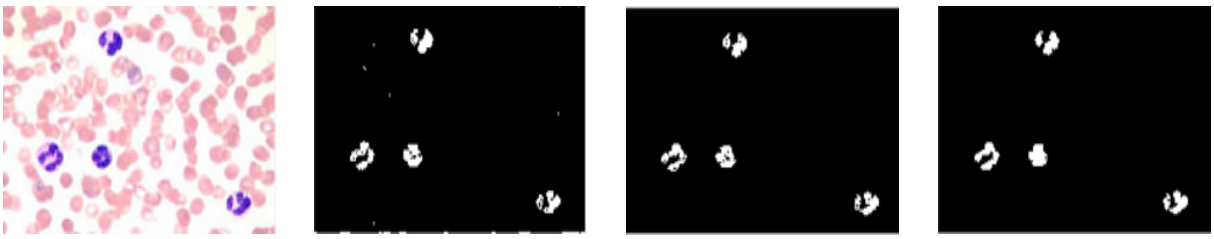

(a) Original image (b) Proposed algorithm (c) Denoising (d) Hole filling

Fig. 4. Nuclear extraction process

2.4 Cytoplasmic Extraction

Selection of color model. The color model selection is similar to that of the nucleus and is selected by observing the different components of the different color models. In Fig. 3(c), the H component of the HSV color model can distinguish the location of WBCs, and the effect of clustering segmentation is greatly improved.

WBCs extraction. After segmentation of the improved FWSA-KM cluster, the small area of the WBCs is extracted and the present small noise particles are corrected by using de-noising algorithm again. Meanwhile, the extracted WBCs will also have the holes and some missing edges, for this purpose, we then use the holes filling and expansion to restore the morphological structure of WBCs.

For the WBCs that are adhered together, we first segment them with the proposed algorithm, and then divide the adhesion part again using the watershed segmentation algorithm, as shown in Fig. 5:

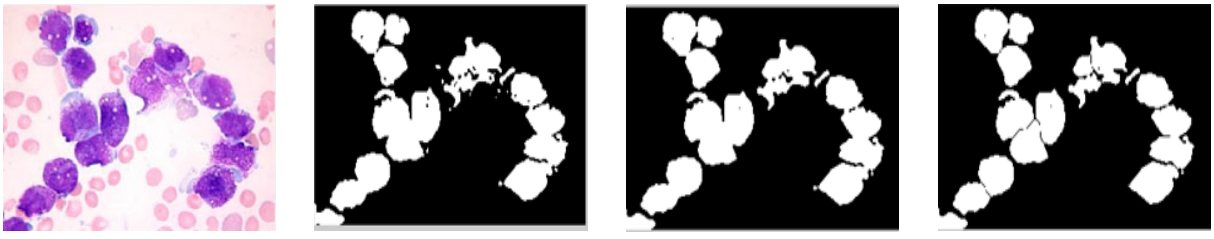

(a) Original image (b) Proposed algorithm (c) Denoising (d) Watershed segmentation

Fig. 5. Touching white blood cells segmentation

Cytoplasmic extraction. Cytoplasmic segmentation is the most difficult part of the WBCs division, because the color of the cytoplasm and that of the WBCs or the background looks quite similar. So the WBCs subtracted from the white cell nucleus, getting part of the cytoplasm, and then returned to color map.

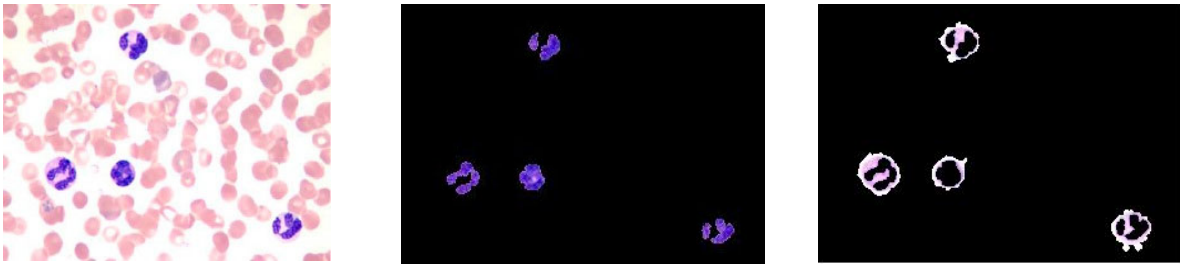

(a) Original image (b) Extraction of nucleus (c) Extraction of cytoplasm

Fig. 6. Cytoplasmic extraction process

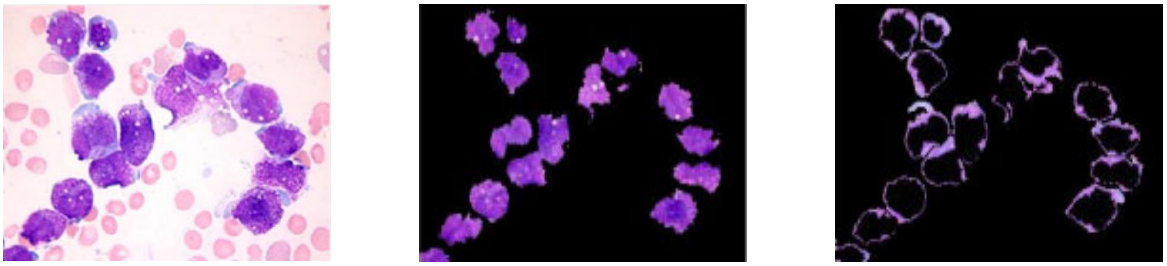

(a) Original image (b) Extraction of nucleus (c) Extraction of cytoplasm

Fig. 7. Cytoplasmic extraction process

3 Experimental Results and Analysis

3.1 Experimental Results

Single or discrete WBCs. In this paper, two sets of data were used in the experiment. The first group of data is obtained from the First Affiliated Hospital of Fujian Medical University. The experimental smears were prepared through conventional methods in the hospital and stained with Wright staining. All WBCs collected from the peripheral blood and bone marrow cell images were identified and classified by laboratory specialists. In the cell image acquisition, an OLYMPUS BX51 microscope and a Nikon high-performance color digital camera were used. The blood smears were observed under microscope 100 times. The field of vision was located in the area where the WBCs were concentrated, and then transferred to the camera mode. The microscope was used to fine-tune the WBCs to the appropriate position of the image. Finally, the digital camera was used to take cell images. Collected images of peripheral blood and bone marrow cells are RGB color images with a resolution of 2080 * 1542. The second set of data is downloaded from the ALL-IDB dataset [21]. These JPEG images are available in RGB format with three resolutions: 2592 * 1944, 1712 * 1368,1226 * 652.

In order to verify the practicability of this algorithm, different types of peripheral blood and bone marrow cell images were tested, and some representative images were extracted for further analysis.

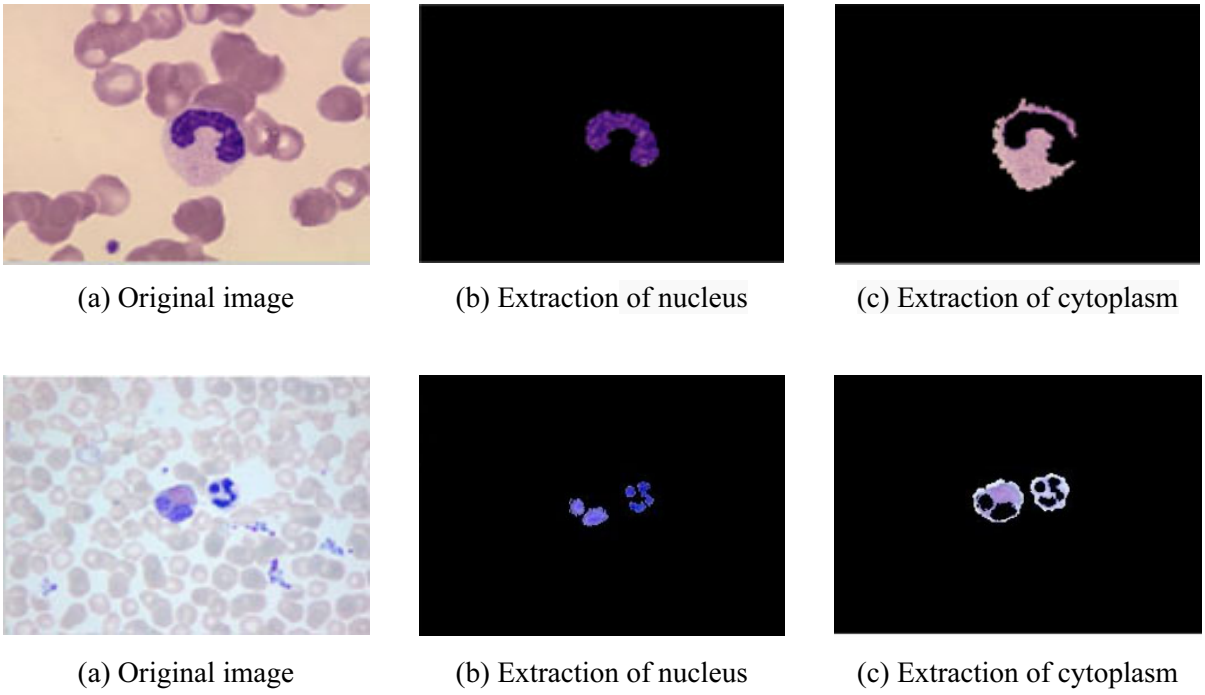

(a) Original image (b) Extraction of nucleus (c) Extraction of cytoplasm

(a) Original image (b) Extraction of nucleus (c) Extraction of cytoplasm

Fig. 8. Single or discrete leukocyte extraction process

Adhesion of WBCs. For the nucleus and cytoplasm color contrast darker, the extracted nuclear morphology is basically correct. And when the contrast is insufficiently strong, some of the segmentation error will occur, as shown in Fig. 9.

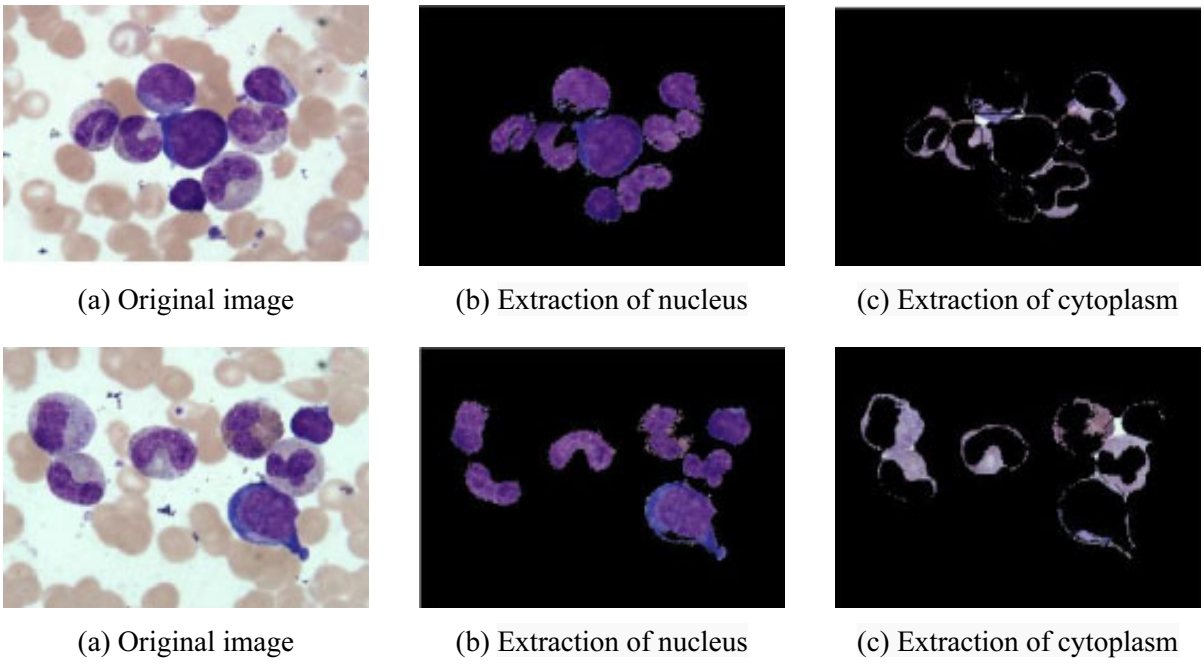

(a) Original image (b) Extraction of nucleus (c) Extraction of cytoplasm

(a) Original image (b) Extraction of nucleus (c) Extraction of cytoplasm

Fig. 9. Touching leukocyte extraction process

Nucleus extraction errors are mainly concentrated in the cytoplasm and nuclei of small contrast cells. For some helical or lobulated nucleis, the basic shapes can be extracted. The error of the cytoplasm is mainly concentrated in the contrast higher cells of the cytoplasm and nucleus, and the chroma of the cytoplasm and the red blood cell are similar.

In short, the morphological extraction of the nucleus can be extracted basically, and cytoplasm

extraction is somewhat inadequate. In addition, single or discrete WBCs extraction will be better than the adhesion of the WBCs. In the case of poor contrast, it is relatively easy to generate a segmentation error.

3.2 Experimental Analysis

Several methods for segmenting leukocytes have been proposed, but most of these methods only apply to a certain class of images. The background color and dyeing conditions of the cell images are different in different databases. Some images in the database were segmented by the algorithm above, and the segmentation results were compared with the results of manual segmentation ("gold standard") to verify the accuracy of the method. In this database, nucleus segmentation obtained an average overall accuracy of 95.81% and 91.28% for cytoplasmic segmentation.

In order to evaluate the performance of the algorithm, Table 1 lists the experimental results, wherein R1 represents the ratio of the number of correctly detected WBCs to the total number of detected WBCs (Equation (14)). When R1 = 1 indicates that the detected WBCs are all correct WBCs, no error detection occurs. The evaluation parameter R2 represents the ratio between the number of detected WBCs and the total number of WBCs, as shown in equation (15). When R2 = 1, no error detection occurs. Equation (16) shows a calculation method for the error detection rate (E1) and the leak detection rate (E2). Evaluation parameters R1 and R2 indicate the accuracy of the segmentation algorithm in detecting WBCs. In the evaluation of R1 and R2, the coincidence accuracy between the segmentation result and the original cell is not considered. That is, there is a certain error between the automatic segmentation result and the "gold standard", as long as the algorithm can locate the approximate position of WBCs. The parameter D, that represents the Hausdorff distance between the boundary of the automatic segmentation result and the expert's manual segmentation result, is used to evaluate the coincidence accuracy of the segmentation result and the original cell, namely the coincidence rate between the segmentation result and the real result. The parameter D also represents the performance of the segmentation result, which is closely related to the final recognition rate (because the feature extraction is highly dependent on the accuracy of the segmentation) and is therefore an important evaluation index. The smaller the parameter D is, the closer the segmentation result is to the "gold standard".

Table 1. Performance evaluation

Parameter	GVF Snake	Ref. [2]	Ref. [10]	Proposed algorithm
R1	91.3%	94.6%	94.87%	96.73%
R2	88%	95.1%	95.6%	97.2%
D	29.7	19.13	18.96	18.02

$$R1 = \frac{The\ number\ of\ correctly\ detected\ WBCs}{Total\ number\ of\ detected\ WBCs} \times 100\% \quad . \tag{14}$$

$$R2 = \frac{Total\ number\ of\ detected\ WBCs}{Total\ number\ of\ WBCs\ that\ existed\ in\ all\ images} \times 100\% \, . \tag{15}$$

$$\begin{cases} E1 = 1 - R1 \\ E2 = 1 - R2 \end{cases} . \tag{16}$$

Fig. 10 shows the segmentation results for individual WBC. Fig. 11 shows the segmentation results for multiple WBCs.

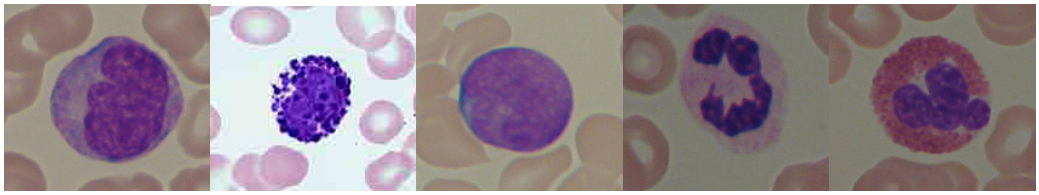

(a) Original image

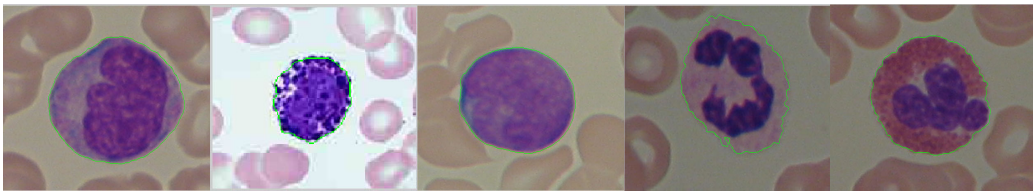

(b) Artificial segmentation

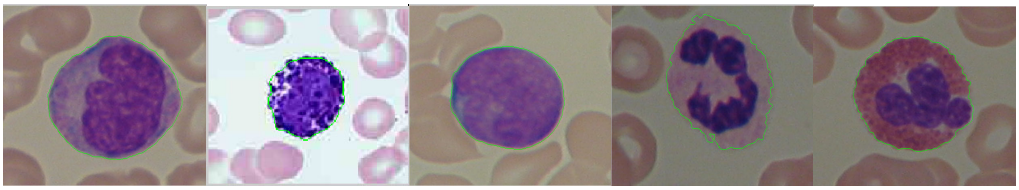

(c) Proposed segmentation algorithm

Fig. 10. Single white blood cell segmentation

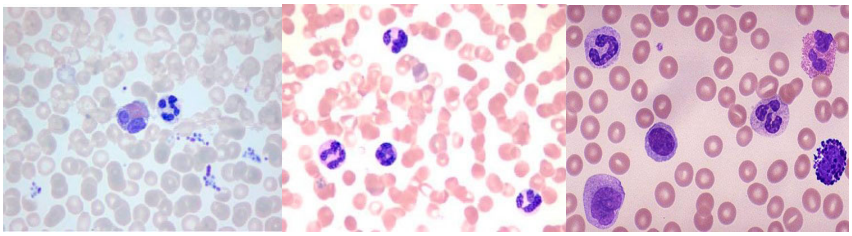

(a) Original image

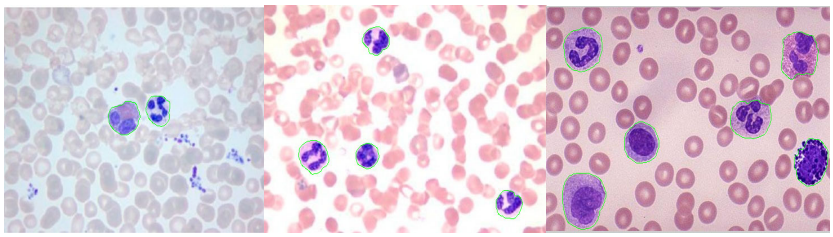

(b) Artificial segmentation

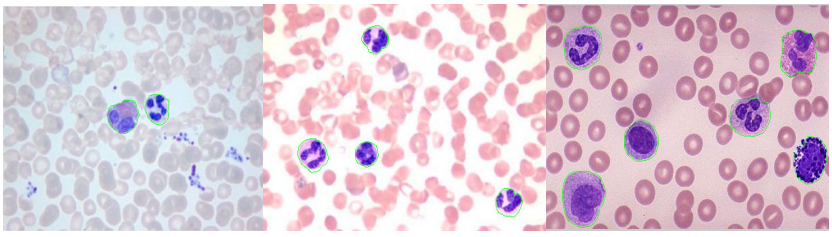

(c) Proposed segmentation algorithm

Fig. 11. Multiple WBCs segmentation

As shown in Table 1, the proposed method has a low detection error rate and lossing rate, and the tracking boundary obtains high accuracy.

The performance comparisons in Table 2 are evaluated by the parameters OR, UR, ER, and RDE. Here OR, UR and ER, denote the over-segmentation rate, under-segmentation rate and the overall error rate, respectively, which are often used to evaluate the performance of segmentation algorithms. RDE represents the relative distance error, which was first proposed by Yang-Mao et al. [22] to evaluate the segmentation results. Assuming that $e_1, e_2, e_3, \cdots, e_n$ is the pixel of E and $t_1, t_2, t_3, \cdots, t_n$ is the pixel of T, where E is the result of segmentation, T is the "gold standard" and n_e and n_t are the number of pixels of E and T, respectively, then RDE is defined as follows:

Table 2. Performance evaluation via average error measure of OR, UR, ER and RDE

Parameter	GVF snake	Ref. [2]	Ref. [10]	Proposed algorithm
OR	0.081	0.063	0.06	0.05
UR	0.075	0.067	0.063	0.056
ER	0.189	0.143	0.12	0.08
RDE	6.30	1.52	1.59	1.36

$$RDE = \frac{1}{2}\left(\sqrt{\frac{1}{n_e}\sum_{i=1}^{n_e} d_{e_i}^2} + \sqrt{\frac{1}{n_t}\sum_{j=1}^{n_t} d_{t_j}^2}\right). \tag{17}$$

$$\begin{aligned} d_{ei} &= \min\left\{distance(e_i, t_j) \middle| j = 1,2,...n_t\right\}, d_{tj} \\ &= \min\left\{distance(e_i, t_j) \middle| i = 1,2,...n_e\right\} \end{aligned}. \tag{18}$$

$distance(e_i, t_j)$ is the Euclidean distance between e_i and t_i.

In Table 2, this method is only slightly worse in terms of UR evaluation, has similar properties to the watershed method in OR evaluation, but performs better on other indicators. At the same time, the proposed algorithm achieves a higher total error rate (8%) and a lower relative distance error (1.36) than the other methods. The performance shows that the proposed algorithm performs better overall.

4 Conclusion

We have proposed to use an improved FWSA K-means clustering algorithm to extract complex and adherent WBCs. Before segmenting the WBCs, the color space conversion is performed. And the accuracy of segmentation can be improved. When the cell image of the RGB color space is converted into the HSI color space, a feature that facilitates the division of the WBCs turns up. The experimental results show that the performance evaluation parameters of R1 and R2 are 96.73% and 97.2% respectively. Furthermore, the experimental results also show that the proposed algorithm has high accuracy, low false positive rate and false detection rate for segmenting the nucleus and cytoplasm. The precision of the WBCs boundary localization is more accurate than that with other algorithms. Therefore, the proposed algorithm is accurate and efficient for the segmenting WBCs in peripheral blood cells and bone marrow cells, and has better performance than traditional methods. Certainly, our proposed algorithm is not perfect. Some limitations also exsit. It cannot detect all the WBCs for some complex cell images and it sometimes regards a few non-WBCs as WBCs. Adhesion segmentation for the diagnosis of complicated abnormal cells in bone marrow diseases remains a great challenge. Hence, how to find a more effective detection method based on our method is the direction of our study in the future.

References

[1] X. Zheng, Y. Wang, G. Wang, White blood cell segmentation using expectation-maximization and automatic support vector machine learning, Data Acquis. Process 28(2013) 614-619.

[2] W. X. Wang, P.Y. Su, Blood cell image segmentation on color information and GVF snake for leukocyte classification on SVM, Optics and Precision Engineering 20(12)(2012) 2781-2790.

[3] B.C. Ko, J.W. Gim, J.Y. Nam, Automatic white blood cell segmentation using stepwise merging rules and gradient vector flow snake, Micron 42(2011) 695-705.

[4] X. Zheng, Y. Wang, G. Wang, A novel algorithm based on visual saliency attention for localization and segmentation in rapidly-stained leukocyte images, Micron 56(2014) 17-28.

[5] C. Pan, D.S. Park, S. Yoon, Leukocyte image segmentation using simulated visual attention, Expert Syst.Appl 39(2012) 7479-7494.

[6] C. Pan, D.S. Park, Y. Yang, Leukocyte image segmentation by visual attention and extreme learning machine, Neural Comput 21(2012) 1217-1227.

[7] C.C. Zhang, X. Xiao, X. Li, White blood cell segmentation by color-space-based K-means clustering, Sensors 14(2014) 16128-16147.

[8] S. Arslan, E. Ozyurek, C.D. Gunduz, A color and shape based algorithm for segmentation of white blood cells in peripheral blood and bone marrow images, Cytom 85(2014) 480-490.

[9] J.s. Lao, K. Chamnongthai, Acute leukemia classification by using SVM and K-Means clustering, in: Proc. the International Electrical Engineering Congress, 2014.

[10] N.M. Salem, Segmentation of white blood cells from microscopic images using K-means clustering, in: Proc. the 31st IEEE National Radio Science Conference, 2014.

[11] Z. Liu, J. Liu, X.Y. Xiao, Segmentation of white blood cells through nucleus mark watershed operations and mean shift clustering, Sensors 15(2015) 22561-22586.

[12] J.W. Zhao, M.S. Zhang, Z.H. Zhou, Automatic detection and classification of leukocytes using convolutional neural networks, Medical & Biological Engineering & Computing (2016) 1-15.

[13] V. Perumal, Fuzzy C means detection of leukemia based on morphological contour segmentation, Procedia Computer Science 58(2015) 84-90.

[14] H.S. Syed, I.U. Arif, N. Saeeda, Efficient leukocyte segmentation and recognition in peripheral blood image, Technology and Health Care 24(2016) 335-347.

[15] L.B. Dorini, R. Minetto, N.J. Leite, Semiautomatic white blood cell segmentation based on multiscale analysis, IEEE Journal of Biomedical and Health Informatics 17(1)(2013) 250-256.

[16] P.K. Mondal, U.K. Prodhan, M.S. Al Mamun, Segmen-tation of white blood cells using fuzzy C means segmentation algorithm, IOSR Jornal of Computer Engineering 1(6)(2014) 1-5.

[17] K.A. Eldahshan, M.I. Youssef, E.H. Masameer, M.A. Mustafa, Segmentation framework on digital microscope images for acute lymphoblastic leukemia diagnosis based on HSV color space, International Journal of Computer Applications 90(7)(2014) 48-51.

[18] K.A. Eldahshan, M.I. Youssef, E.H. Masameer, M.A. Hassan, Comparison of segmentation framework on digital microscope images for acute lymphoblastic leukemia diagnosis using RGB and HSV color spaces, Journal of Biomedical Engineering and Medical Imaging 2(2)(2015) 26-34.

[19] V. Singhal, P. Singh, Correlation based feature selection for diagnosis of acute lymphoblastic leukemia, in: Proc. the 3rd ACM International Symposium on Women in Computing and Informatics (WCI'15), 2015.

[20] W.H. Fu, L.F. Ma, A.L. Li, Blind estimation of underdetermined mixing matrix based on improved K-means clustering,

Systems Engineering and Electronic 36(11)(2014) 2143-2147.

[21] ALL-IDB Website. Available online: http://www.dti.unimi.it/fscotti/all (accessed on 23 July 2015).

[22] S.F. Yang-Mao, Y.K. Chan, Y.P. Chu, Edge enhancement nucleus and cytoplast contour detector of cervical smear Images, IEEE Trans. Syst. Man Cybern, Part B 38(2008) 353-366.